JBC Papers in Press. Published on May 12, 2020 as Manuscript RA119.012043
The latest version is at https://www.jbc.org/cgi/doi/10.1074/jbc.RA119.012043

Tripartite-motif family protein 35-28 regulates microglia development by preventing necrotic death of microglial precursors in zebrafish

Tao Yu[1], Haoyue Kuang[1], Jiahao Chen[2], Xi Lin[3], Yi, WU[1]; Keyu Chen[4], Mingjie Zhang[1,3,4], Wenqing Zhang[2*], and Zilong Wen[1,3,4*]

Running title: Regulation of microglia development by a *trim35* orthologue

Keywords: Trim, zebrafish, microglia, development, cell death, macrophage, immune system, central nervous system (CNS), genetic screen, neuronal inflammation

[1]Shenzhen Key Laboratory for Neuronal Structural Biology, Biomedical Research Institute, Shenzhen Peking University - The Hong Kong University of Science and Technology Medical Center, Shenzhen 518036, China

[2]Department of Cell, Developmental and Integrative Biology, School of Medicine, South China University of Technology, Guangdong, Guangzhou 510630, China.

[3]Division of Life Science, State Key Laboratory of Molecular Neuroscience, Center of Systems Biology and Human Health, Hong Kong University of Science and Technology, Clear Water Bay, Kowloon, Hong Kong, China.

[4]Greater Bay Biomedical Innocenter, Shenzhen Bay Laboratory，Shenzhen 518055, China

*Correspondence should be addressed to:
WQZ: Department of Cell, Developmental and Integrative Biology, School of Medicine, South China University of Technology, Guangzhou 510630, China.
ZLW: Division of Life Science, State Key Laboratory of Molecular Neuroscience, Center of Systems Biology and Human Health, Hong Kong University of Science and Technology, Clear Water Bay, Kowloon, Hong Kong, China. Tel: (852)2358-7294; Fax: (852)2358-1552; Email: zilong@ust.hk

Microglia are tissue-resident macrophages in the central nervous system (CNS) that play essential roles in the regulation of CNS development and homeostasis. Yet, the genetic networks governing microglia development remain incompletely defined. Here, we report the identification and characterization of a microglia-defective zebrafish mutant *wulong*^{hkz12} (*wul*^{hkz12}) isolated from an ethylnitrosourea (ENU)-based genetic screen. We show that *wul*^{hkz12} mutants harbors a missense point mutation in the gene region encoding the PRY/SPRY domain of the tripartite-motif family protein 35-28 (*trim35-8*) gene. Time-lapse imaging revealed that the loss of Trim35-28 function causes lytic necrosis of microglial precursors/peripheral macrophages, as indicated by cytoplasmic swelling and membrane rupture of these precursors and accompanied by neutrophil infiltration and systemic inflammation. Intriguingly, the lytic necrosis of microglial precursors in *trim35-28*–deficient mutants appeared to depend neither on the canonical pyroptotic nor on necroptotic pathways, as inhibition of the key component in each pathway could not rescue the microglia phenotype in *trim35-28*-deficient mutants. Finally, results from tissue-specific rescue experiments suggested that Trim35-28 acts cell-autonomously in the survival of microglial precursors. Taken together, the findings of our study reveal Trim35-28 as a regulatory protein essential for microglia development.

Microglia are the central nervous system (CNS)-resident macrophages, and they play essential roles in regulating the homeostasis of the CNS. As the key immune cells in the CNS, microglia, upon brain infection or brain injury, are quickly activated and migrate to the target site and remove infectious agents and cellular debris, leading to the elimination and resolving of detrimental neuronal inflammation (1-3). In addition to functioning as scavengers, recent studies have indicated that microglia also actively participate in the regulation of synaptic pruning and neuronal activity (4-6). It is therefore not surprising that the aberrant function of microglia has been implicated to be closely associated with the onset and progression of many neurodegenerative disorders, such as Alzheimer's disease, Parkinson disease and multiple sclerosis (7-9). Unlike the neuroectodermal origin of other cell types in the CNS, microglia are of hematopoietic origin (8-10). Fate mapping studies have revealed that microglia in mice are derived from hematopoietic precursors generated in a single origin, the yolk sac (YS) (11-13), whereas microglia in zebrafish arise from two sources, the rostral blood island (RBI) and the aorta-gonad mesonephros (AGM) (14). Despite the difference in terms of their origins, the developmental regulation of microglia appears to be evolutionarily conserved between fish and mice, as microglia in both organisms undergo similar developmental steps that are governed by a highly conserved repertoire of regulators, including Pu.1 (14-16), Irf8 (17, 18) and Csf1r (19, 20). Yet, the molecular networks controlling the formation of microglia remain incompletely defined. Although recent advance of the CRISPR-Cas system has made reverse genetic study much feasible in zebrafish model (21), an unbiased

forward genetic study with this tiny organism will still provide a useful tool to identify new players involving in various biological processes.

For a long time, apoptosis has been thought to be the only form of programmed cell death governed by well-defined intrinsic molecular pathways program (22). However, emerging evidences have suggested that necrosis, although initially described as accidental cell death, can be programed by defined signaling pathways, including the receptor-interacting serine/threonine-protein kinases (RIPKs) dependent necroptosis and inflammasome-mediated pyroptosis (23-25). Apoptosis and necrosis can be easily distinguished based on their morphological changes of the dying cells. While the morphological changes of apoptosis involve chromosome fragmentation, membrane blebbing and shrinkage of cell volume, necrosis, either accidental or programed, display a common morphological feature - cytoplasmic swelling due to early loss of membrane integrity (23-25). Another conspicuous difference between apoptosis and necrosis is their distinct immunological consequences. Through packaging the cellular contents within membrane-bound cell apoptotic bodies, apoptosis does not trigger inflammation. On the other hand, necrosis is a lytic cell death that causes the release of cellular contents and the exposure of pathogen-associated molecular patterns and danger-associated molecular patterns, resulting in the induction of inflammation (23, 25, 26). Despite numerus elegant studies showing that apoptosis and anti-apoptosis mechanism play an essential role in cell lineage development and organ formation (27, 28), the role of necrosis and anti-necrosis mechanism in cell and organ development remains less explored.

The TRIM proteins comprise a large family of proteins defined by the presence of RBCC motif, which has a tandem organization of a RING domain, one or two B-box domains and a coiled-coil domain (29-31). The RING domain of the TRIM family proteins possesses E3 ubiquitin ligase activity, which has been shown to be crucial for mediating their effects on innate immunity. The B-box domains are zinc- binding motifs facilitating the recognition of the viral and intracellular proteins during innate response to viral infection. And the coiled-coil domain mediates homomeric and heteromeric interactions among TRIM family members and with other proteins to form high molecular complexes essential for the generation of innate immunity. TRIM35, a member in the class IV of TRIM family protein (32), is structurally characterized by the association of RBCC motif with the C-terminal PRYSPRY domain (also known as B30.2 domain). Although TRIM35 was initially cloned as a tumor suppressor gene (33) and a downstream factor of M-CSF signaling involving in apoptosis (34), a recent study has revealed that TRIM35 appears to inhibit the TLR7/9-mediated type I interferon production via ubiquitination and degradation of IRF7 (35). In zebrafish, 37 members of Trim35 paralogues have been identified (36), and little is known about their functions *in vivo*.

In this study, we described the isolation and characterization a microglia defective zebrafish mutant *wul*^{hkz12} and uncovered the role of Trim35-28, a member of Trim35 orthologues, as an anti-necrosis factor during microglia development.

Results

wul^{hkz12} mutants are defective in microglia and microglial precursors

To uncover novel factors involving in microglia development, we carried out an ENU-based forward genetic screen searching for microglia defective zebrafish mutants (19). A mutant designated as *wul*^{hkz12} (*wulong* is the name of a Chinese tea) was identified because of the lack of neutral red (NR) staining in the developing brain at 3 days post-fertilization (dpf) and 6 dpf (Fig. 1*A*). Because of the nature of NR staining, the absence of NR signals in the brain of *wul*^{hkz12} mutants could be caused by the impairment of the lysomsomal function of microglia or the loss of microglia population. To distinguish these two possibilities, we performed whole-mount in situ hybridization (WISH) with the microglial marker apolipoprotein Eb (*apoeb*) and the pan-leukocyte marker lymphocyte cytosolic protein 1 (Lcp1). Results showed that, while *apoeb*$^{+}$ and Lcp1^{+} cells were abundantly present in the brains of control siblings, these cells were nearly absent in *wul*^{hkz12} mutants (Fig. 1*B*). These data suggest that the lack of NR staining in *wul*^{hkz12} mutants is likely attributed to the loss of microglia.

Interestingly, we noticed that, although microglia were largely absent in the brains of *wul*^{hkz12} mutants, a significant number of Lcp1^{+} leukocytes accumulated in the periphery (data not shown). To define the nature of the peripheral Lcp1^{+} cells, we monitored the formation of peripheral macrophages and neutrophils at 4 dpf, both of which are known to be Lcp1^{+} (37), with lineage-specific markers. Results showed that the number of peripheral macrophages was significantly reduced in *wul*^{hkz12} mutants (data not shown). In contrast, Sudan Black B (SB) staining, a dye that preferentially stains neutrophils (38), revealed a robust increase of neutrophils in the mutants (Fig. 1*C*). Notably, the increased neutrophils in *wul*^{hkz12} mutants were found to be scattered in the tissues, such as yolk sac and trunk regions, where normally devoid of neutrophils in wild-type (WT) siblings (Fig. 1*C*). Moreover, neutrophils often formed clusters in the caudal hematopoietic tissue (CHT) in *wul*^{hkz12} mutants (Fig. 1*C*). These data indicate that the *wul*^{hkz12} mutants are lack of microglia and peripheral macrophages but have an expanded neutrophil phenotype in the periphery.

trim35-28 is mutated in *wul*^{hkz12} mutants

To identify the gene mutated in *wul*^{hkz12} mutants, we carried out positional cloning analysis. The *wul* mutation was mapped to a 200 kb region on chromosome 16 flanked by two simple sequence length polymorphism (SSLP) markers, SSLP65 and SSLP82 (Fig. 2*A*). DNA Sequencing of the coding regions of the 10 candidate genes within this 200 kb region revealed a T to A missense mutation in the sixth exon of the *trim35-28* gene, leading to a single amino acid substitution from Isoleucine (I) to Asparagine (N) at position 454 in the PRYSPRY (B30.2) domain (Fig. 2*B*).

To confirm that the I454N mutation in the *trim35-28* locus is responsible for the mutant phenotype, we designed a *trim35-28* morpholino (MO) to test whether knocking down Trim35-28 expression in WT zebrafish would produce a phenotype similar to that of *wul*^{hkz12} mutants. As expected, results showed that *trim35-28* MO knockdown caused a severe reduction of microglia in zebrafish (<5 microglia, n=63/88; 5~15 microglia, n=20/88 in morphants; >20 microglia in control embryos, n=69/69)

(Fig. 2*C*). We then performed the rescue experiment with *in vitro* synthesized WT or I454N *trim35-28* mRNA. Consistent with the MO knockdown assay, we showed that the injection of WT but not I454N mutant *trim35-28* mRNA could partially rescue the microglia number in *wul*^{hkz12} mutants (Fig. 2, *D-E*). Collectively, these data demonstrate that *trim35-28* is indeed the causative gene responsible for the loss of microglia in *wul*^{hkz12} mutants.

We were next keen to investigate how this I454N mutation disrupts the function of Trim35-28 protein. We first aligned the protein sequences of zebrafish Trim35-28 PRY/SPRY domain with four known PRYSPRY domains sharing the highest degree of similarity with Trim25-28 from the Protein Data Bank (PDB). Results indicated that their the PRY/SPRY domains had a highly conserved secondary structure (Fig. S1*A*), indicating that the PRY/SPRY domain of Trim35-28 is likely to adopt a similar folding pattern with the canonical PRY/SPRY domains. We then took the human PYRIN PRY/SPRY domain (PDB ID: 2wl1) (39) as a core structure to model the structure of the Trim35-28 PRY/SPRY domain (Fig. S1*C*). We found that I_{454} in Trim35-28 appeared to corresponding to I_{755} in human PYRIN (Fig. S1*B*, indicated by red arrow), which locates in a scaffolding beta-strand (Beta-strand 12) (39) and is buried in a hydrophobic core (Fig. S1*C*, blue dashed circle). The two loops (loop 2 and loop 5 in PYRIN) covering this hydrophobic core are the key components of the pocket essential for target recognition (40). The importance of this binding pocket is further documented by the observation that several mutations in the Familial Mediterranean fever patients are found to locate on the wall or near the rim of the target-binding pocket (39, 40) (Fig. S1*C*, labeled with red letters). Given the fact that the I454N mutation had no obvious effect on the stability and subcellular location of the proteins (Fig. S1, *D* and *E*), we believe that the substitution of hydrophobic Isoleucine to hydrophilic Asparagine at residue 454 might cause a conformational change of these two loops, resulting in the disruption of this protein function.

Trim35-28 is cell-autonomously required for microglia development

Having shown that *trim35-28* is the causative gene mutated in *wul*^{hkz12} mutants, we next asked whether the loss of microglia phenotype and the neutrophil expansion phenotype in the mutants was caused by a cell-autonomous or non-cell-autonomous mechanism. To test that, we firstly examined the temporal-spatial expression expressions of *trim35-28* during early zebrafish development. WISH analysis showed that *trim35-28* transcripts were ubiquitously expressed, with a relative enrichment in the developing brain and pharyngeal arches (Fig. S2). The ubiquitous expression of *trim35-28* raises the possibility that the microglia and neutrophil phenotype in *wul*^{hkz12} mutants may not be necessary caused by a cell-autonomous mechanism. To clarify this issue, we generated two transgenic lines, *Tg(mpeg1:trim35-28)* and *Tg(lyz:trim35-28)*, in which the expression of WT *trim35-28* was under the control of the macrophage-specific gene 1 (*mpeg1*) promoter (41) and the neutrophil-specific lysozyme C (*lyz*) promoter (42) respectively (Fig. 3*A*). These transgenic lines were outcrossed with *wul*^{hkz12} mutant fish to test whether the restoration of WT *trim35-28* expression in a lineage-specific manner could rescue the

microglia and neutrophil defect in *wul*^{hkz12} mutants. Results showed that forced expression of *trim35-28* in the mutants with the *mpeg1* promoter could fully rescue the microglia phenotype (Fig. 3, *B* and *C*). Interestingly, the neutrophil phenotype was also rescued in this macrophage-specific *trim35-28* expression *Tg(mpeg1:trim35-28);wul*^{hkz12} line (Fig. 3, *D-E*). In contrast, both phenotypes could not be restored in the neutrophil-specific *trim35-28* expression *Tg(lyz:trim35-28);wul*^{hkz12} line (Fig. 3, *B-E*). Taken together, these results indicate that *trim35-28* is cell-autonomously required for the development of microglia and their precursors and the expansion of neutrophils in *wul*^{hkz12} mutants is a secondary effect caused by the defect of microglia.

Accelerated necrotic cell death of microglial precursors in periphery accounts for the loss of microglia and expansion of neutrophils in wul^{hkz12} mutants

To dissect the cellular mechanism underlying the loss of microglia in *wul*^{hkz12} mutants, we examined the formation of microglial precursors – peripheral macrophages at early developmental stages. WISH of microfibril associated protein 4 (*mfap4*) expression revealed that peripheral macrophages were specified and distributed properly in *wul*^{hkz12} mutants at 36 hpf (Fig. 4*A*, upper panel). However, by 2.5 dpf, macrophage number in mutant embryos was significantly reduced (Fig. 4*A*, lower panel; Fig.4*B*), suggesting that the loss of microglia in *wul*^{hkz12} mutants is largely due to the impairment of microglial precursors in periphery prior to their invasion and colonization of the brain. To define which cellular mechanism, accelerated cell death or impaired proliferation, caused the reduction of microglial precursors in *wul*^{hkz12} mutants, we performed terminal deoxynucleotidyltransferase-mediated dUTP nick end labeling (TUNEL) staining and bromodeoxyuridine (BrdU) incorporation assay. As shown in Figure 4*C* and 4*D*, compared to the rare cell death in siblings, massive TUNEL signals were detected in *wul*^{hkz12} mutants and the majority of those signals co-localized with macrophage-specific marker *mpeg1*-GFP, suggesting that microglial precursors undergo accelerated cell death in the mutants. In contrast, BrdU incorporation assay showed comparable proliferation rate of microglial precursors between the mutants and siblings (Fig. S3, *A* and *B*). Taken together, these results demonstrate that the loss of microglia in *wul*^{hkz12} mutants is largely ascribed to the excessive death of microglial precursors in the periphery.

To define the nature of the death of the mutant microglial precursors, we performed time-lapse imaging to monitor the morphological and behavioral changes of the microglial precursors in the mutants and siblings from 2 dpf to 3 dpf, at which these precursors were shown to actively undergo cell death. We found that a substantial number of *mpeg1*$^{+}$ cells in *wul*^{hkz12} mutants underwent cell death as indicated by their fragmentation (Fig. 5, *A* and *B*). Notably, unlike the typical morphological changes (cytoplasmic shrinkage and membrane blebbing) in the apoptotic macrophages induced by metronidazole (Mtz) treatment of *Tg(mpeg1:Gal4;uas:nfsB-mCherry)* embryos (Fig. S4*A* and Movie S1) (43-45), the dying *mpeg1*$^{+}$ cells in *wul*^{hkz12} mutants displayed distinctive morphology and behavior including

retraction of processes and increase of cytoplasm volume (Fig. 5*A*, a'1-a'2; a''1-a''4 and Movie S2) followed by rapid cell membrane rupture and fragmentation into multiple small pieces (Fig. 5*A*, *a'3-a'7* and *a''5-a''7* and Movie S2). To prove that the death of microglial precursors in *wul*^{hkz12} mutants was indeed not apoptosis, we examined the generation of activated Caspase 3, a well-known apoptosis marker, by immunostaining with specific antibody. Results showed that, while the activated Caspase 3 was robustly detected in the apoptotic neurons in the brains of 2.5 dpf *wul*^{hkz12} mutants (Fig. S4*B*), it was completely absence in the *mfap4*-GFP^{+} microglial precursors (Fig. S4*C*). These data indicate that the death of *mpeg1*$^{+}$ cells in *wul*^{hkz12} mutants is not apoptosis but rather is necrosis. Indeed, the death of *mpeg1*$^{+}$ cells in *wul*^{hkz12} mutants was always coupled with the infiltration of neutrophils (Fig. 5*B*, *b6-b7*, dashed circles and Movie S3) and the expression of pro-inflammatory cytokines such as *il-1β*, *tnfα* and *il-6* (Fig. 5, *C* and *D*) as well as the macrophage activation marker *irg1* (Fig. S5) in mutant microglial precursors. Altogether, these results indicate that the death of microglial precursors in *wul*^{hkz12} mutants resembles the characteristics of lytic necrosis, including cytoplasm swelling, membrane rupture and induction of inflammation (23, 25).

Lytic necrosis of microglial precursors in wul^{hkz12} mutants is mediated by neither the canonical pyroptotic nor necroptotic signaling pathways

Previous studies have shown that the loss of function mutations in the nucleotide oligomerization domain (NOD)-like receptor *nlrc3-like* cause the pyroptotic death of microglia and their precursors due to the hyperactivation of inflammasome pathway (46, 47). As the phenotypes observed in *wul*^{hkz12} and *nlrc3-like* mutants are similar, we hypothesized that the disruption of Trim35-28 function might also lead to the aberrant activation of the inflammasome pathway, resulting in the pyroptotic death of microglia and peripheral macrophages. To test this hypothesis, we outcrossed *wul*^{hkz12} mutants with *asc*$^{\Delta 31}$ fish, in which the key component of apoptosis-associated speck-like protein containing a caspase recruitment domain (Asc) is inactivated, thereby abolishing the activation of the canonical inflammasome pathway (47). Surprisingly, we found that the microglia number in *wul*^{hkz12}*;asc*$^{\Delta 31}$ double mutants was comparable to that in *wul*^{hkz12} single mutants (Fig. 6, *A* and *B*), suggesting that the death of microglial precursors in *wul*^{hkz12} mutants is independent of the canonical pyroptotic pathway. To further support this notion, we employed MOs to knock down the expression of *gsdmea* and *gsdmeb*, two zebrafish counterparts of mammalian *gasdermin* family genes essential for pyroptosis (47) and asked whether it would rescue the mutant phenotype. Consistent with the observation in *wul*^{hkz12}*;asc*$^{\Delta 31}$ double mutants, knocking down *gsdmea* or *gsdmeb* in *wul*^{hkz12} mutants failed to rescue the microglia phenotype (Fig. 6, *C* and *D*), indicating that the lytic necrosis of microglial precursors in *wul*^{hkz12} mutants is not a typical pyroptotic cell death. We therefore speculated that the lytic necrosis of microglial precursors in *wul*^{hkz12} mutants could be necroptosis. To test this hypothesis, we generated a *ripk3*$^{\Delta 52}$ mutant fish, in which the function of Ripk3, a key component involving in necroptosis (48, 49) is disrupted (Fig. S6). The mutant fish were outcrossed with *wul*^{hkz12} mutants to test whether the inactivation of Ripk3 could

rescue the microglia phenotype in *wul*^{hkz12} mutants. Surprisingly, results showed that the loss of Ripk3 function could not rescue the microglia phenotype in *wul*^{hkz12} mutants (Fig. 6, *E* and *F*). Taken together, these results indicate that the lytic necrosis of microglial precursors in *wul*^{hkz12} mutants is likely not mediated by the canonical pyroptotic and necroptotic pathways.

Discussion

In this report, we demonstrate that zebrafish *trim35-28*, a member of *trim* family, is essential for the formation of microglia in the CNS by inhibiting necrosis-like cell death of microglial precursors/macrophages.

Since there are 37 members of *trim35* genes in the zebrafish genome, an interesting question is why zebrafish acquire such large number of *trim35* family genes. Based on their evolutionary dynamics, Sardiello et al (50) and Boudinot et al (36) have classified that teleost *trim* genes into two distinct subclasses. The first subclass includes the *trim* family genes containing 1 or 2 fish paralogues corresponding to the mammalian counterparts, and this family of *trim* genes is thought to carry out conserved functions across species. On the other hand, the members of second subclass are highly-expanded *trim* genes including *trim35* family, in which the C-terminal PRY/SPRY domains, which define their substrate specificity, are likely to be evolved under a positive selection mechanism (36). Hence, we speculate that this unique evolutionary pathway may endow each zebrafish *trim35* gene with specific function, thereby facilitating the adaption of zebrafish to their unique adequate milieu. Indeed, protein sequence alignment indicates that the PRY/SPRY domains of Trim35-28 shares only 30%-40% similarities with other Trim35 proteins and its mammalian counterparts (data not shown), suggesting that the functions of Trim35-28 may not be substituted by the other members of the Trim35 family and its mammalian counterpart. This idea is supported by the observations that *trim35-28*-deficient mutants die at around 10 dpf and forced expression of mammalian TRIM35 fails to rescue the mutant phenotype (data not shown). Thus, it would be interesting to explore the roles of other *trim35* members as well as its mammalian counterpart.

Another intriguing finding is that inactivation of the key players in pyroptotic (Asc and Gasdermin) and necroptosis (Ripk3) pathway fails to rescue the death of microglial precursors/macrophages in *wul*^{hkz12} mutants, despite microglial precursors/macrophages in *trim35-28*-deficient mutants undergo typical characteristics of necrotic cell death. These results could be explained by several mechanisms. One possible mechanism is the complementary effect caused by the activation of the genetic compensation response. Recent studies have shown that premature termination codon-bearing mRNA could trigger genetic compensation response via Upf3a and COMPASS components (51, 52). It is therefore reasonable to speculate that the *asc*$^{\Delta 31}$ and *ripk3*$^{\Delta 52}$ mutations, both of which generate premature termination codon-bearing mRNA, may activate the genetic compensation response pathways, resulting in the complementary effect on the blockage of pyroptotic and necroptosis pathway. However, our preliminary study showed that the elimination of the genetic compensation response pathway by MO knockdown of *upf3a* expression (47, 48) could not

rescue microglia defects in *wul*^{hkz12}*;asc*$^{\Delta 31}$ or *wul*^{hkz12}*;ripk3*$^{\Delta 52}$ double mutants (data not shown), suggesting that the activation of genetic compensation response is likely not to be the mechanism. An alternative mechanism is that the *trim35-28*-deficient microglial precursors/macrophages undergo pyroptosis or necroptosis through an Asc-independent or a Ripk3-idenpendent mechanism. Finally, the death of microglial precursors/macrophages in *wul*^{hkz12} mutants may represent another type of cell death which has not been well characterized. Further in-depth analysis will be required to define the nature of the death of *trim35-28*-deficient microglial precursors/macrophages and the underlying molecular basis.

Experimental procedures

Zebrafish husbandry and ENU mutagenesis

Zebrafish were maintained according to standard protocol (53). AB and WIK wild-type, *wul*^{hkz12}, *pycard*$^{\Delta 31}$ (47), *ripk3*$^{\Delta 52}$, *myd88* (54), *Tg(mpeg1:loxP-DsRedx-loxP-eGFP)hkz015Tg* (55), *Tg(mpeg1:Gal4), Tg(uas:nfsB-mCherry)(56), Tg(mfap4:eGFP)020Tg, Tg(mpeg1:trim35-28)hkz030Tg, Tg(lyz:trim35-28)hkz031Tg* and *Tg(mpeg1:loxP-eGFP)hkz032Tg* were used in this study. The ENU (Sigma) mutagenesis was carried out as described (57, 58). All experiments were conducted with approval of the Animal Ethics Committee of the Hong Kong University of Science and Technology and the Animal Ethics Committee of Shenzhen Peking University-The Hong Kong University of Science and Technology Medical Center.

Sequential Neutral Red and Sudan Black B staining

NR staining (14) were conducted first and then the embryos were separated into two pools based on the microglia phenotype for subsequent SB staining (38).

Positional cloning

Positional cloning was performed as described previously (59). In brief, *wul*^{hkz12} mutation was first mapped to linkage group 16 by two SSLP markers z10036 and z4670. Two closer markers, z25218 and z17383 (one for each direction) were then chosen to screen embryos for fine mapping. By analyzing 2548 total meiosis events, *wul*^{hkz12} mutation was narrowed down to a 200 kb region with two SSLP markers, BX571757.8-sslp65 (1 recombinant out of 2548 total meiosis) and CR391910.16-sslp82 (1 recombinant out of 2528 total meiosis). Sequencing of the coding regions of candidate genes revealed a T to A missense mutation in the last exon of *trim35-28*. The primers used for positional cloning of *wul*^{hkz12} mutation are listed as follows: BX571757.8-sslp65:5'-TCAGCTTCTGCATGGAAACA-3'/5'-TGGCAGTCTCTCAC-TGTTGTG-3';CR391910.16-sslp82: 5'-CAAAAATAGCAGCAACCCACA-3'/5'- CGC-CTTGCCTTCATTTAATC-3'. The primers used for *trim35-28* sequencing are: *trim35-28*-F1 5'-GAAAGCGAAACTATAGCTCGG-3'; *trim35-28*-R1 5'- GTTGATGAGGG -CTCCGTTAAC-3'; *trim35-28*-F2 5'-CATCGGTCGTGACATCACAGG-3'; *trim35-28*-R2 5'-GACTCTTACGCGTTGTCATTTG-3'.

Morpholinos (MOs)

trim35-28 ATG MO:5'-TCACTGCTATCTGCCATGTCGGATC-3'; *gsdmea sp* MO: 5'-TCATAGTGTTTCCTAACCTTCCTCT

-3'; *gsdmeb* ATG MO: 5'-TGCAAACATCTTCAATGCTGACAAG-3' were designed and synthesized by Gene Tools. 2 nl *trim35-28* ATG MO (1 mM) or *gsdmea sp* MO (0.5 mM) or *gsdmeb* ATG MO (0.25 mM) was injected into 1-cell stage embryos.

In vitro mRNA synthesis

WT and mutant *trim35-28* cDNA were cloned into PCS2(+) plasmid. The resulting constructs were linearized by NotI digestion and the *trim35-28* mRNA were synthesized using mMESSAGE mMACHINE™ SP6 Transcription Kit (AM1340) according to manufacturer's instruction.

In-vitro synthesis of antisense RNA probes and WISH

Antisense RNA probes and WISH were performed according to standard protocol (53).

Generation of transgenic lines

The 4 kb *mpeg1* promoter (41) and 2.4 kb *lyz* promoter (42) was cloned into the pBluescript II SK(+) vector containing two arms of Tol2 sequences to drive *trim35-28* expression in macrophages and neutrophils respectively. The *-4kbmpeg1:trim35-28* or *-2.4kblyz:trim35-28* construct, together with transpose mRNA, was injected into 1-cell stage fertilized embryos. The injected embryos were then raised to adult for germline transmission screening.

Acridine orange, BrdU incorporation and TUNEL staining

Acridine orange (AO) staining was performed according to manufacturer's instruction. BrdU incorporation assay and TUNEL staining was performed as previously reported (60).

Time-lapse imaging and images

Time-lapse imaging was performed under Leica SP8 confocal microscopy with 20 x HC PL APO 203/0.70 DRY objective according to the protocol described previously (61). Images of fluorescent signals and immuno-staining were captured by Leica SP8 confocal microscope and Zeiss LSM 710 confocal microscope.

Statistics

Statistics were analyzed using the two-tailed Student's t test. Result was considered significant if $p < 0.05$. Values represent Mean ±SD.

Data availability

All data presented in this paper are contained within the article.

Acknowledgments

The authors thank Dr. Hae-Chul Park for providing the *Tg(uas:nfsB-mCherry)* line.

Funding

This work was supported by the Natural Science Foundation of Guangdong Province (2018A030313149), Shenzhen Science and Technology Innovation Committee (JCYJ20180223181227269), China Postdoctoral Science Foundation Grant (2017M620379), National Natural Science Foundation of China (31801211), Research

Grants Council of the HKSAR (16131916; 16103718; N_HKUST621/17; C6002-17GF; AoE/M-09/12, and T13-605/18-W), and Innovation and Technology Commission of the HKSAR (ITCPD/17-9).

Author contributions

T.Y., H.K., J.C., X.L., Y.W. designed the research, performed experiments, and analyzed data; K.C. performed bioinformatic analysis of PRY/SPRY domain; M.Z., W.Z. and Z.W. designed the research and analyzed data.

Conflict of interest

The authors declare that they have no conflicts of interest with the contents of this article.

References

1. Gomez-Nicola, D., and Perry, V. H. (2015) *The Neuroscientist* **21**, 169-184
2. Hristovska, I., and Pascual, O. (2016) *Frontiers in Integrative Neuroscience* **9**
3. Davalos, D., Grutzendler, J., Yang, G., Kim, J. V., Zuo, Y., Jung, S., Littman, D. R., Dustin, M. L., and Gan, W. B. (2005) *Nature neuroscience* **8**, 752-758
4. Paolicelli, R. C., Bolasco, G., Pagani, F., Maggi, L., Scianni, M., Panzanelli, P., Giustetto, M., Ferreira, T. A., Guiducci, E., Dumas, L., Ragozzino, D., and Gross, C. T. (2011) *Science* **333**, 1456-1458
5. Stevens, B., Allen, N. J., Vazquez, L. E., Howell, G. R., Christopherson, K. S., Nouri, N., Micheva, K. D., Mehalow, A. K., Huberman, A. D., Stafford, B., Sher, A., Litke, A. M., Lambris, J. D., Smith, S. J., John, S. W., and Barres, B. A. (2007) *Cell* **131**, 1164-1178
6. Li, Y., Du, X.-f., Liu, C.-s., Wen, Z.-l., and Du, J.-l. (2012) *Developmental cell* **23**, 1189-1202
7. Glass, C. K., Saijo, K., Winner, B., Marchetto, M. C., and Gage, F. H. (2010) *Cell* **140**, 918-934
8. Prinz, M., Priller, J., Sisodia, S. S., and Ransohoff, R. M. (2011) *Nature neuroscience* **14**, 1227-1235
9. Prinz, M., and Priller, J. (2014) *Nat Rev Neurosci* **15**, 300-312
10. Ransohoff, R. M., and Cardona, A. E. (2010) *Nature* **468**, 253-262
11. Ginhoux, F., Greter, M., Leboeuf, M., Nandi, S., See, P., Gokhan, S., Mehler, M. F., Conway, S. J., Ng, L. G., Stanley, E. R., Samokhvalov, I. M., and Merad, M. (2010) *Science* **330**, 841-845
12. Kierdorf, K., Erny, D., Goldmann, T., Sander, V., Schulz, C., Perdiguero, E. G., Wieghofer, P., Heinrich, A., Riemke, P., Holscher, C., Muller, D. N., Luckow, B., Brocker, T., Debowski, K., Fritz, G., Opdenakker, G., Diefenbach, A., Biber, K., Heikenwalder, M., Geissmann, F., Rosenbauer, F., and Prinz, M. (2013) *Nature neuroscience* **16**, 273-280
13. Schulz, C., Gomez Perdiguero, E., Chorro, L., Szabo-Rogers, H., Cagnard, N., Kierdorf, K., Prinz, M., Wu, B., Jacobsen, S. E., Pollard, J. W., Frampton, J., Liu, K. J., and Geissmann, F. (2012) *Science* **336**, 86-90
14. Xu, J., Zhu, L., He, S., Wu, Y., Jin, W., Yu, T., Qu, J. Y., and Wen, Z. (2015) *Developmental cell* **34**, 632-641
15. Jin, H., Li, L., Xu, J., Zhen, F., Zhu, L., Liu, P. P., Zhang, M., Zhang, W., and Wen, Z. (2012) *Blood* **119**, 5239-5249

16. Yu, T., Guo, W., Tian, Y., Xu, J., Chen, J., Li, L., and Wen, Z. (2017) *Blood* **129**, 509-519
17. Li, L., Jin, H., Xu, J., Shi, Y., and Wen, Z. (2011) *Blood* **117**, 1359-1369
18. Shiau, C. E., Kaufman, Z., Meireles, A. M., and Talbot, W. S. (2015) *PloS one* **10**, e0117513
19. Herbomel, P., Thisse, B., and Thisse, C. (2001) *Developmental biology* **238**, 274-288
20. Wu, S., Xue, R., Hassan, S., Nguyen, T. M. L., Wang, T., Pan, H., Xu, J., Liu, Q., Zhang, W., and Wen, Z. (2018) *Developmental cell* **46**, 552-563.e554
21. Sun, Y., Zhang, B., Luo, L., Shi, D.-L., Wang, H., Cui, Z., Huang, H., Cao, Y., Shu, X., Zhang, W., Zhou, J., Li, Y., Du, J., Zhao, Q., Chen, J., Zhong, H., Zhong, T. P., Li, L., Xiong, J.-W., Peng, J., Xiao, W., Zhang, J., Yao, J., Yin, Z., Mo, X., Peng, G., Zhu, J., Chen, Y., Zhou, Y., Liu, D., Pan, W., Zhang, Y., Ruan, H., Liu, F., Zhu, Z., Meng, A., and Consortium, Z. (2019) *Genome research* **30**, 118-126
22. Lockshin, R. A., and Zakeri, Z. (2001) *Nature reviews. Molecular cell biology* **2**, 545-550
23. Wallach, D., Kang, T.-B., Dillon, C. P., and Green, D. R. (2016) *Science* **352**
24. Vandenabeele, P., Galluzzi, L., Vanden Berghe, T., and Kroemer, G. (2010) *Nat Rev Mol Cell Bio* **11**, 700-714
25. Lamkanfi, M. (2011) *Nature reviews. Immunology* **11**, 213-220
26. Wallach, D., Kang, T.-B., and Kovalenko, A. (2014) *Nature reviews. Immunology* **14**, 51-59
27. Pérez-Garijo, A., and Steller, H. (2015) *Development* **142**, 3253-3262
28. Kristiansen, M., and Ham, J. (2014) *Cell Death & Differentiation* **21**, 1025-1035
29. Khan, R., Khan, A., Ali, A., and Idrees, M. (2019) *Reviews in Medical Virology* **29**, e2028
30. Hatakeyama, S. *Trends in biochemical sciences* **42**, 297-311
31. Ozato, K., Shin, D.-M., Chang, T.-H., and Morse Iii, H. C. (2008) *Nature Reviews Immunology* **8**, 849
32. Short, K. M., and Cox, T. C. (2006) *Journal of Biological Chemistry* **281**, 8970-8980
33. Lalonde, J.-P., Lim, R., Ingley, E., Tilbrook, P. A., Thompson, M. J., McCulloch, R., Beaumont, J. G., Wicking, C., Eyre, H. J., Sutherland, G. R., Howe, K., Solomon, E., Williams, J. H., and Klinken, S. P. (2004) *Journal of Biological Chemistry* **279**, 8181-8189
34. Kimura, F., Suzu, S., Nakamura, Y., Nakata, Y., Yamada, M., Kuwada, N., Matsumura, T., Yamashita, T., Ikeda, T., Sato, K., and Motoyoshi, K. (2003) *Journal of Biological Chemistry* **278**, 25046-25054
35. Wang, Y., Yan, S., Yang, B., Wang, Y., Zhou, H., Lian, Q., and Sun, B. (2015) *FEBS letters* **589**, 1322-1330
36. Boudinot, P., van der Aa, L. M., Jouneau, L., Du Pasquier, L., Pontarotti, P., Briolat, V., Benmansour, A., and Levraud, J.-P. (2011) *PloS one* **6**, e22022
37. Meijer, A. H., van der Sar, A. M., Cunha, C., Lamers, G. E. M., Laplante, M. A., Kikuta, H., Bitter, W., Becker, T. S., and Spaink, H. P. (2008) *Developmental & Comparative Immunology* **32**, 36-49
38. Le Guyader, D., Redd, M. J., Colucci-Guyon, E., Murayama, E., Kissa, K., Briolat, V., Mordelet, E., Zapata, A., Shinomiya, H., and Herbomel, P. (2008) *Blood* **111**, 132-141
39. Weinert, C., Grütter, C., Roschitzki-Voser, H., Mittl, P. R. E., and Grütter, M. G. (2009) *Journal of molecular biology* **394**, 226-236
40. Woo, J.-S., Suh, H.-Y., Park, S.-Y., and Oh, B.-H. (2006) *Molecular cell* **24**, 967-976
41. He, S., Chen, J., Jiang, Y., Wu, Y., Zhu, L., Jin, W., Zhao, C., Yu, T., Wang, T., Wu, S., Lin, X., Qu, J. Y., Wen, Z., Zhang, W., and Xu, J. (2018) *eLife* **7**, e36131
42. Kitaguchi, T., Kawakami, K., and Kawahara, A. (2009) *Mechanisms of development* **126**, 314-323
43. FELMER, R. N., and CLARK, J. A. (2004) *Biological Research* **37**, 449-460
44. Curado, S., Anderson, R. M., Jungblut, B., Mumm, J., Schroeter, E., and Stainier, D. Y. R. (2007) *Developmental Dynamics* **236**, 1025-1035

45. Curado, S., Stainier, D. Y. R., and Anderson, R. M. (2008) *Nature protocols* **3**, 948-954
46. Shiau, Celia E., Monk, Kelly R., Joo, W., and Talbot, William S. (2013) *Cell reports* **5**, 1342-1352
47. Wang, T., Yan, B., Lou, L., Lin, X., Yu, T., Wu, S., Lu, Q., Liu, W., Huang, Z., Zhang, M., Zhang, W., and Wen, Z. (2019) *Journal of Genetics and Genomics*
48. Sun, L., Wang, H., Wang, Z., He, S., Chen, S., Liao, D., Wang, L., Yan, J., Liu, W., Lei, X., and Wang, X. (2012) *Cell* **148**, 213-227
49. Li, D., Meng, L., Xu, T., Su, Y., Liu, X., Zhang, Z., and Wang, X. (2017) *eLife* **6**, e27692
50. Sardiello, M., Cairo, S., Fontanella, B., Ballabio, A., and Meroni, G. (2008) *BMC evolutionary biology* **8**, 225
51. Ma, Z., Zhu, P., Shi, H., Guo, L., Zhang, Q., Chen, Y., Chen, S., Zhang, Z., Peng, J., and Chen, J. (2019) *Nature* **568**, 259-263
52. Rossi, A., Kontarakis, Z., Gerri, C., Nolte, H., Hölper, S., Krüger, M., and Stainier, D. Y. R. (2015) *Nature* **524**, 230
53. Westerfield, M. (2000)
54. van der Vaart, M., van Soest, J. J., Spaink, H. P., and Meijer, A. H. (2013) *Disease Models and Mechanisms* **6**, 841-854
55. Xu, J., Wang, T., Wu, Y., Jin, W., and Wen, Z. (2016) *Developmental cell* **38**, 214-222
56. Ah-Young, C., Pan-Soo, K., Suhyun, K., Eunmi, K., Dohyun, K., Inyoung, J., Hwan-Ki, K., Jae-Ho, R., Cheol-Hee, K., June, C., Jin-Ho, S., and and Hae-Chul, P. (2013) *Molecules and cells* **36**, 82-87
57. Solnica-Krezel, L., Schier, A. F., and Driever, W. (1994) *Genetics* **136**, 1401-1420
58. Mullins, M. C., Hammerschmidt, M., Haffter, P., and Nüsslein-Volhard, C. (1994) *Current Biology* **4**, 189-202
59. Zhou, Y., and Zon, L. I. (2011) Chapter 16 - The Zon Laboratory Guide to Positional Cloning in Zebrafish. in *Methods in cell biology* (Detrich, H. W., Westerfield, M., and Zon, L. I. eds.), Academic Press. pp 287-309
60. Li, X., Lan, Y., Xu, J., Zhang, W., and Wen, Z. (2012) *Development* **139**, 4321-4329
61. Zhen, F., Lan, Y., Yan, B., Zhang, W., and Wen, Z. (2013) *Development* **140**, 3977-3985

The abbreviations used are: CNS, central nervous system; WUL, wulong; ENU, ethylnitrosourea; TRIM, tripartite motif family; YS, yolk sac; RBI, rostral blood island; AGM, aorta-gonad mesonephros; RIPK, receptor-interacting serine/threonine-protein kinase; NR, neutral red; DPF, days post-fertilization; WISH, whole-mount in situ; CHT, caudal hematopoietic tissue; APOEB, apolipoprotein Eb; LCP1, lymphocyte cytosolic protein 1; SB, Sudan black B; WT, wild-type; SSLP, simple sequence length polymorphism; I, isoleucine; N, asparagine; MO, Morpholino; PDB, protein data bank; MPEG1, macrophage-expressed gene 1; LYZ, lysozyme C; MFAP4, microfibril associated protein 4; TUNEL, terminal deoxynucleotidyltransferase-mediated dUTP nick end labeling; BrdU, bromodeoxyuridine; MTZ, metronidazole; NOD, nucleotide oligomerization domain; ASC, apoptosis-associated speck-like protein containing a caspase recruitment domain; AO, acridine orange.

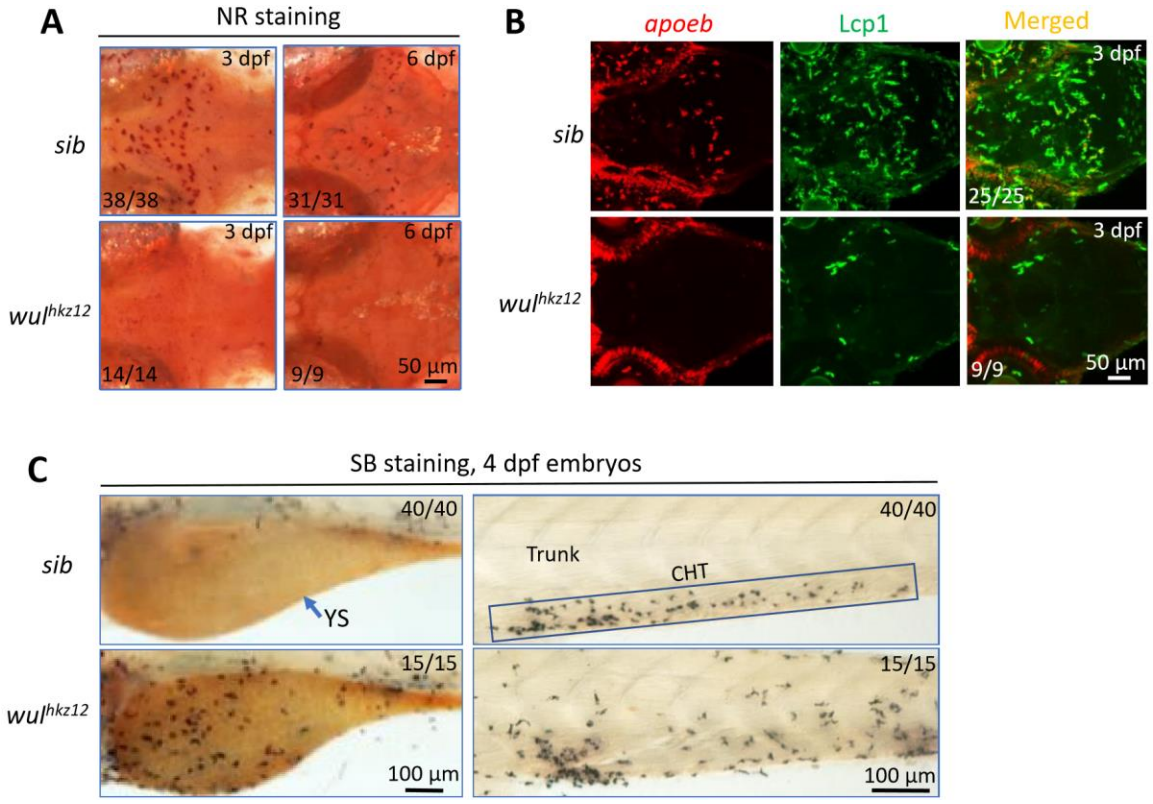

Figure 1. Microglia deficiency and neutrophilia in *wul*^{hkz12} mutants. *A,* NR staining of microglia in siblings and *wul*^{hkz12} at 3 dpf and 6 dpf. *B, apoeb* WISH and Lcp1 antibody staining of microglia in siblings and *wul*^{hkz12} mutants at 3 dpf. Embryos in A and B are in dorsal views with anterior to the left. *C,* SB staining of neutrophils in the YS (left panel) and caudal trunk region (right panel) in 4 dpf siblings and *wul*^{hkz12} mutants. Embryos are in lateral view with anterior to the left.

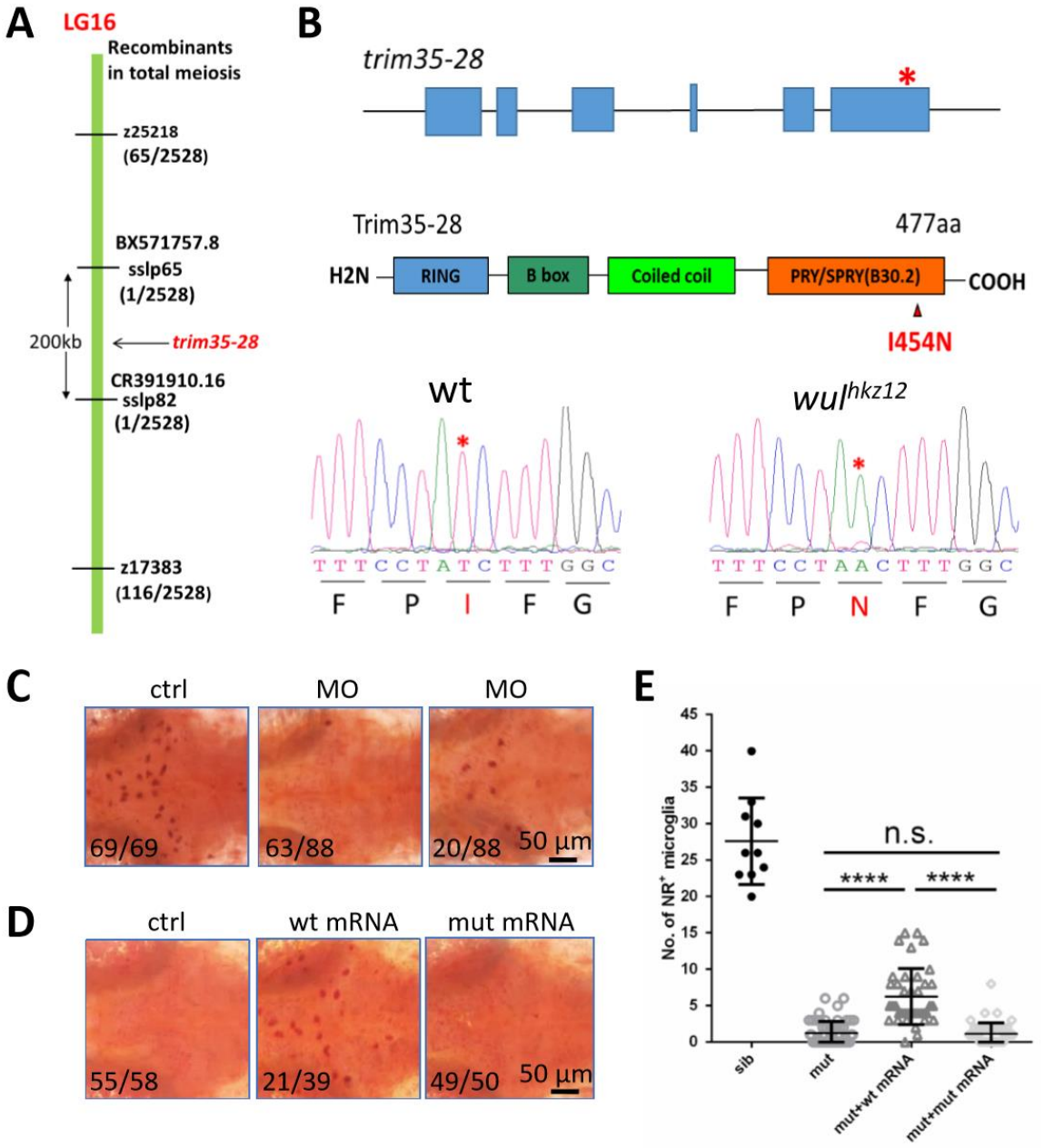

Figure 2. Identification of *wul*^{hkz12} mutant gene. *A,* genetic and physic map of *wul*^{hkz12} locus. The mutation was eventually mapped to a region on Chromosome 16 flanking by two SSLP markers, BX571757.8-sslp65 (1 recombinant out of 2548 total meiosis) and CR391910.16-sslp82 (1 recombinant out of 2528 total meiosis). *B,* schematic view of the *trim35-28* gene locus, protein structure and *wul*^{hkz12} mutation. Chromagrams of cDNA sequence from WT and *wul*^{hkz12} mutants reveal a T to A missense mutation in *trim35-28*, leading to the substitution of amino acid I_{454} by N in the PRY/SPRY(B30.2) domain. *C,* NR staining of microglia in 3 dpf WT control (left) and *trim35-28* MO injected embryos (the middle panel representing MO-injected embryos with 5 or less microglia; the right panel representing MO-injected embryos with 5-15 microglia). *D,* NR staining of microglia in 3 dpf *wul*^{hkz12} mutants (left), *wul*^{hkz12} mutants injected with WT *trim35-28* mRNA

(middle) and mutant *trim35-28* mRNA (right). Embryos are in dorsal views with anterior to the left. *E,* quantification of NR positive microglia in siblings, *wul*^{hkz12} mutants, *wul*^{hkz12} mutants injected with WT *trim35-28* mRNA and *wul*^{hkz12} mutants injected with mutant *trim35-28* mRNA. ****P<.0001. Error bars represent SD.

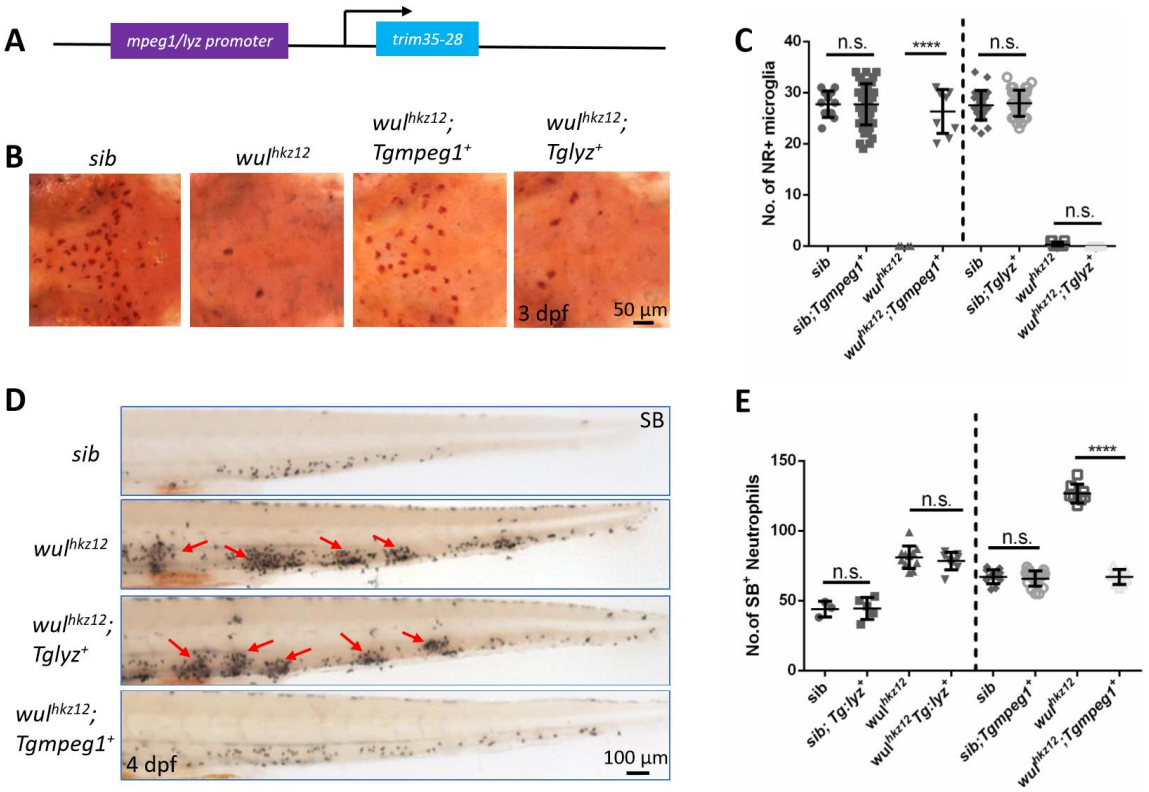

Figure 3. Microglia deficiency and neutrophil expansion in *wul^{hkz12}* mutants was caused by cell-autonomous and none-cell autonomous effect respectively. *A,* schematic view of constructs, in which the expression of *trim35-28* is under the control of the 4.02 kb macrophage-specific *mpeg1* promoter and the 2.4 kb neutrophil-specific *lyz* promoter. *B,* NR staining of microglia in 3 dpf siblings, *wul^{hkz12}* mutants, *wul^{hkz12};Tg(mpeg1:trim35-28)$^{+}$* and *wul^{hkz12};Tg(lyz:trim35-28)$^{+}$* embryos. Embryos are in dorsal views with anterior to the left. *C,* quantification of NR^{+} microglia in each group of panel B. n.s.= not significant, P>0.05; ****P<0.001. Error bars represent SD. *D,* SB staining of neutrophils in 3 dpf siblings, *wul^{hkz12}* mutants, *wul^{hkz12};Tg(mpeg1:trim35-28)$^{+}$* and *wul^{hkz12};Tg(lyz:trim35-28)$^{+}$* embryos. Red arrows indicate neutrophil cluster in CHT. Embryos are in laterally views with anterior to the left. *E,* quantification of SB^{+} Neutrophils in each group of panel D. n.s.=not significant, P>0.05; ****P<0.001. Error bars represent SD.

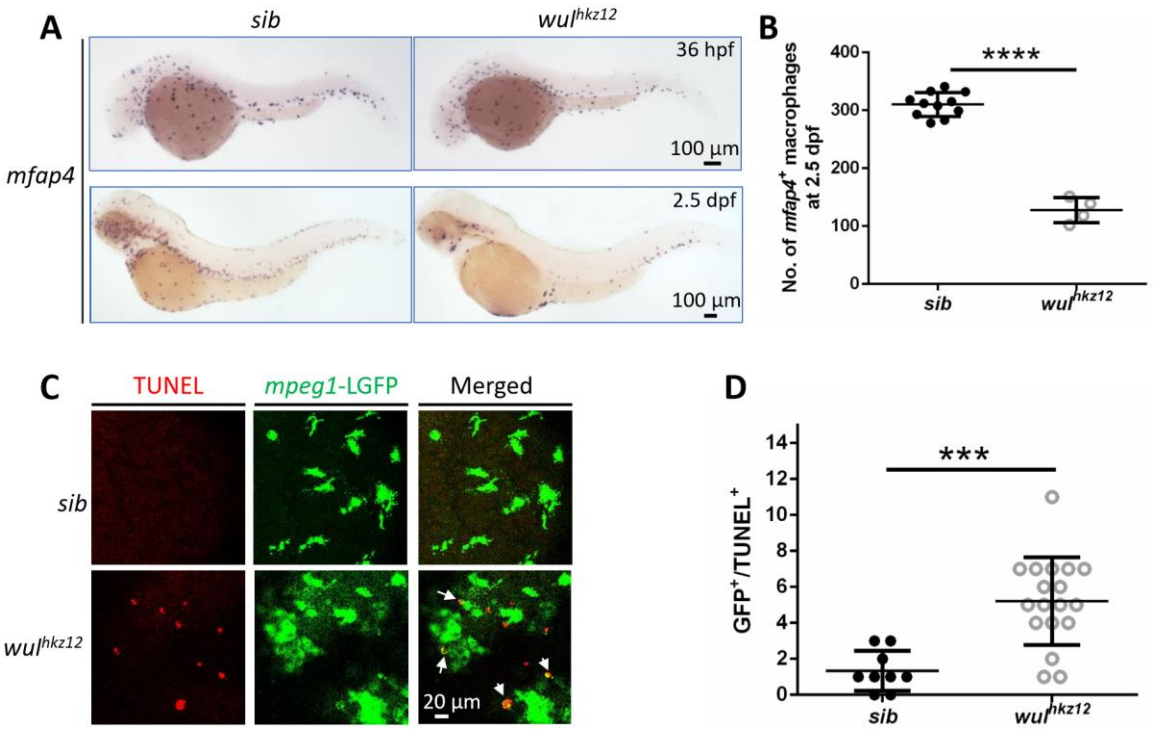

Figure 4. Microglial precursors/macrophages undergo excessive cell death in *wul*^{hkz12} mutants. *A,* WISH of *mfap4* expression in 36 hpf and 2.5 dpf siblings (left) and *wul*^{hkz12} mutants (right). *B,* quantification of mfap4+ macrophages in 2.5 dpf siblings and *wul*^{hkz12} mutants. ****P<0.0001. *C,* co-staining of TUNEL and *mpeg1*-LGFP in the yolk sac region of 2.5 dpf siblings and *wul*^{hkz12} mutants. Embryos are in ventral view with anterior to the left. *D,* quantification of TUNEL^{+}/GFP^{+} cells in siblings and *wul*^{hkz12} mutants. *** P<0.001. Error bars represent SD.

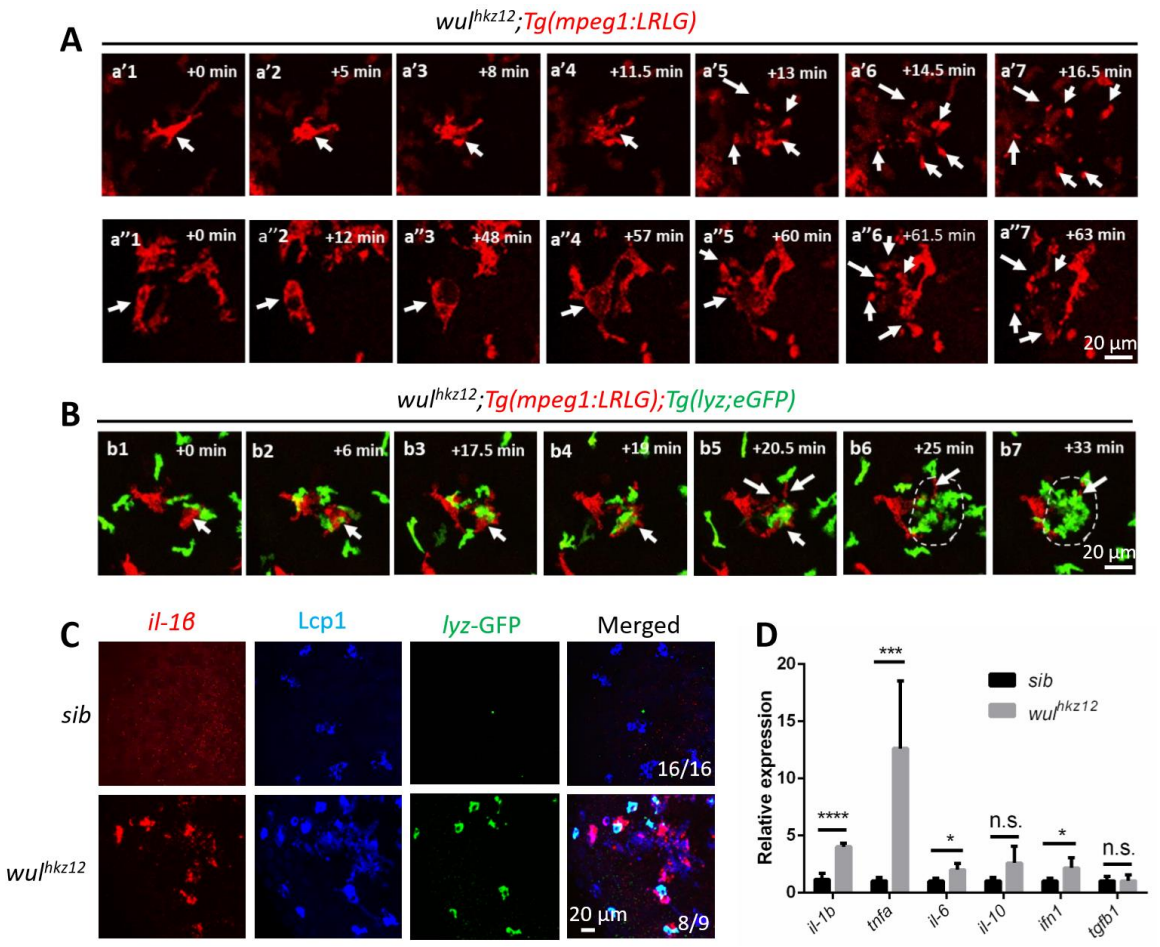

Figure 5. The death of microglial precursors/macrophages in *wul*^{hkz12} mutants resembles necrotic cell death. *A,* time-lapse confocal imaging of a *wul*^{hkz12}*;Tg(mpeg1:LRLG)* embryos from 2.5 dpf to 3.5 dpf. White arrows indicate the swelling and breakdown of two microglial precursors. *B,* time-lapse confocal imaging of a *wul*^{hkz12}*;Tg(mpeg1:LRLG);Tg(lyz:eGFP)* embryo from 2.5 dpf to 3.5 dpf. White arrows indicate a dying microglial precursor and the dash white circle indicates the infiltration of neutrophils. *C,* WISH of *il-1β* expression and co-staining with *lyz*-GFP and Lcp1 antibody in 2.5 dpf siblings and *wul*^{hkz12} mutants. *D,* quantitative RT-PCR of *il-1β, tnfα, il-6, il-10, ifn1* and *tgfb1* expression in 3 dpf siblings and *wul*^{hkz12} mutants. Expression level of target genes was normalized with *elf1a* expression. Error bars represent SD.

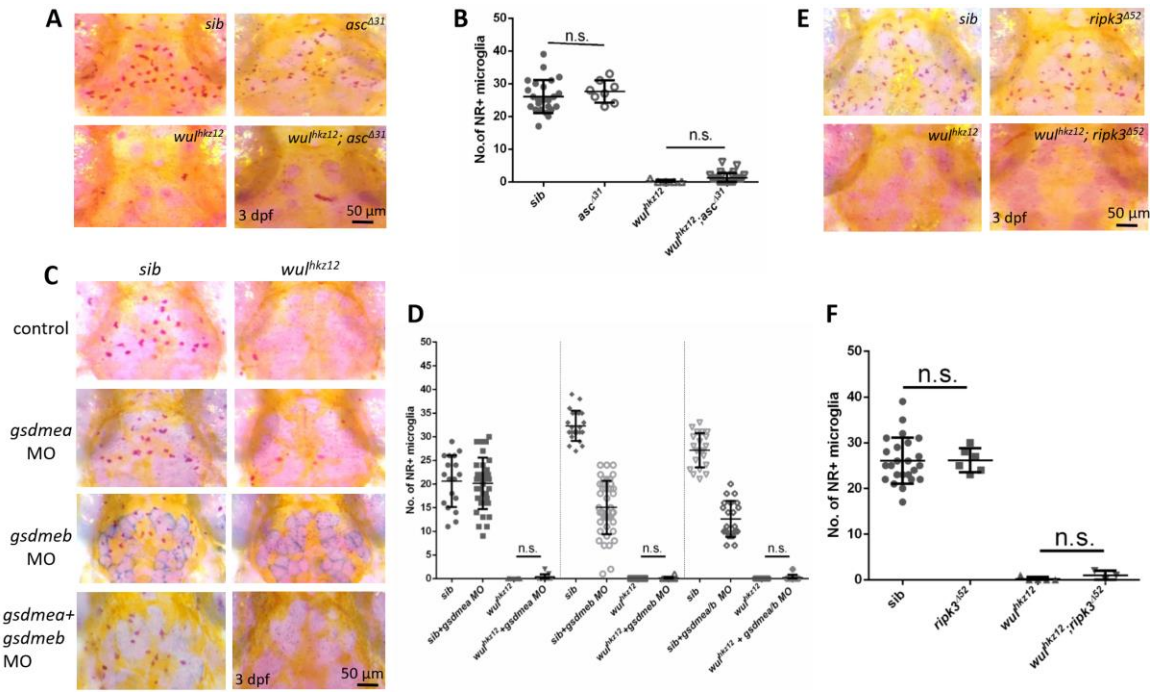

Figure 6. Lytic necrosis of microglial precursors/macrophages in *wul^{hkz12}* mutants is independent of canonical pyroptotic or necroptotic signaling pathways. *A,* NR staining of 3 dpf siblings, *asc^{Δ31}* mutants, *wul^{hkz12}* mutants and *wul^{hkz12};asc^{Δ31}* double mutants. *B,* quantification of NR positive microglia in A. n.s.=not significant P>0.05. *C,* NR staining of 3 dpf siblings, *wul^{hkz12}* mutants, siblings injected *gsdmea* MO, *wul^{hkz12}* mutants injected *gsdmea* MO, siblings injected *gsdmeb* MO, *wul^{hkz12}* mutants injected *gsdmeb* MO, siblings injected with both *gsdmea* and *gsdmeb* MOs and *wul^{hkz12}* mutants injected with both *gsdmea* and *gsdmeb* MOs. *D,* quantification of Neutral Red positive microglia in C. n.s. = not significant, P>0.05. *E,* NR staining of 3 dpf siblings, *ripk3^{Δ52}* mutants, *wul^{hkz12}*mutants and *wul^{hkz12};ripk3^{Δ52}* double mutants. *F,* quantification of NR positive microglia in E. n.s.=not significant P>0.05. Error bars represent SD.

Tripartite-motif family protein 35-28 regulates microglia development by preventing necrotic death of microglial precursors in zebrafish

Tao Yu, Haoyue Kuang, Jiahao Chen, Xi Lin, Yi Wu, Keyu Chen, Mingjie Zhang, Wenqing Zhang and Zilong Wen

J. Biol. Chem. published online May 12, 2020
